Heat Exchanger for Alumina Preheating in Aluminium Reduction Cells

Dagoberto Schubert Severo[1] and Vanderlei Gusberti[2]
1. Director,
2. PhD Engineer
CAETE Engenharia Ltda, Porto Alegre, RS, Brazil
Corresponding author: dagoberto@caetebr.com

Abstract

The raw materials supplied to the aluminium reduction cell need to achieve the process temperature of around 960 °C. The most relevant heat up energy requirement is used to bring alumina temperature from the potroom to the process temperature, consuming around of 0.56 kWh/kg Al. Reducing the process energy requirement by recovering some of the energy loss is fundamental if one is seeking ways to reduce cell specific energy consumption.

One major share of energy wasted at the aluminium reduction cell process is through the hot off-gas collection. A heat exchanger designed to preheat the alumina by using the heat of the gases generated by the reduction process is presented. This device can be used in existing point-feeder prebake cell technologies. Numerical models were used to predict how much energy can be recovered. Around of 0.30 kWh/kg Al of direct heat recovery is predicted using the heat exchanger to preheat alumina. Indirect beneficial side effects open the possibility for a total energy consumption reduction of 1.2 – 1.5 kWh/kg Al.

Keywords: Aluminium electrolysis cells, energy consumption, alumina preheat, energy recovery.

1. Introduction

Reducing the specific energy consumption of aluminium reduction cells is one of the greatest goals of nowadays light metals industry. There are many energy recovery opportunities in the cell that are been employed in smelters. Usually, heat recovery methods and devices [1 – 5] are proposed using the wasted cell energy to heat up an external fluid, and then the thermal energy can be employed in other applications. Sometimes, the heat exchanger has other objectives beyond energy recovery such as decreasing the off-gas temperature before the GTC [2] and the improvement of the emissions capturing efficiency. Other works propose to use wasted energy to heat up the raw materials. Anode preheat is proposed in paper [6] and patent [10] and advantages on the anode current pickup are reported [6].

The concern about alumina preheating has already been seen in earlier publications. US patent 3,006,825 presents an alumina feeder wherein the alumina is preheated by the burners' off-gas in Søderberg cells; the gases passing through an alumina fluidized bed [11]. The feeder disclosed in the US patent 3,371,026 is claimed to have the ability to preheat the alumina before feeding [12].

The Distributed Pot Suction was implemented by Hydro [7, 8], achieving reductions in overall pot off-gas flow, reducing the top energy loss while increasing the gas temperature. This enabled their pots to operate below 11.8 kWh/kg Al [9]. The reported energy saving by using localized gas suction reached up to 0.4 kWh/kg Al. The overall effect might be smaller because the energy loss through other parts of the superstructure tends to increase.

2. Direct and Indirect Benefits of Alumina Preheat

Preheating the alumina fed into the bath has the potential to improve the electrolysis process thermal efficiency through many aspects:

a) Reduction in energy consumption to increase the alumina temperature from ambient to process temperature. It can be calculated from Equation (1) where only sensible heat is considered: ΔH is an integration of specific heat C_p over the heat up temperature limits, no phase change is accounted in this process. Approximately 0.56 kWh/kg Al is required.

$$\Delta H \,\Big|_{25°C}^{960°C} = \int_{25°C}^{960°C} C_p(T)dT \qquad (1)$$

b) Dissolution of preheated alumina is easier than cold alumina. When cold alumina is added heat transfer dominates the dissolution process. The cell current efficiency improves if dissolution is improved, as the cell becomes less prone to muck and alumina concentration in the bath becomes more homogeneous. Each 1 % current efficiency gained represents around 0.14 kWh/kg Al for a typical modern cell with 94 % current efficiency (CE) and specific energy consumption (SEC) of 13.2 kWh/kg Al. This is obtained from derivative of the well-known formula for SE: $\Delta SEC = -(\Delta CE/CE)$ x SEC.

c) The alumina dissolution is an endothermic process. The cell superheat must be high enough to be able to provide energy for heating up and dissolving the alumina. The bath superheat can be understood as an energy reservoir used for this task. When feeding preheated alumina, the cell superheat can be lowered and therefore, heat losses through the sidewalls can be decreased. Figure 1 shows the impact of ambient temperature alumina feeding on the local bath temperature. This was measured in a 150 kA point-fed cell at a distance one and a half anode length from the point feeder, which fed 1.4 kg of alumina every 100 s [13].

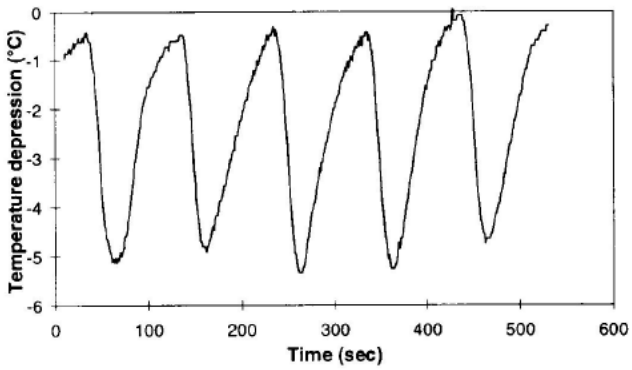

Figure 1. Impact of alumina heat-up and dissolution on local bath temperature [13].

Let us consider a realistic example: a 300 kA cell loses 600 kW through heat dissipation: 50 % from the top, 25 % over the cathode panel and 25 % through side ledge (150 kW). The cell voltage is 4.0 V and energy consumption of 12.5 kWh/kg Al. At the ledge, heat loss Q is proportional to superheat ΔT, ledge area A and heat transfer coefficient h, $Q = hA\Delta T$. If averaged superheat is equal to 10 °C, each degree of superheat lower would mean 15 kW of heat loss saving, which corresponds to 0.16 kWh/kg Al at 94 % current efficiency.

d) The heat exchanger device proposed is accompanied with localized pot suction. This potentially reduces the top heat loss because the under hood space would present lower temperature, reducing convection and radiation heat losses. The total false air suction is around 100 times the cavity gas emission in current standard cell technology. If the suction is localized, the false air gas flow could be greatly reduced to 5 or 10 times the cavity emissions. The literature [9] estimates a potential gain up to 0.4 kWh/kg Al by using localized pot suction.

The combined effects have the potential to reduce the specific energy consumption in 1.2 kWh/kg Al if alumina can be fed at 550 °C, the CE is increased by 1 % and superheat can be lowered by 5 °C. Further reduction could be achieved by the localized pot suction benefits, potentially achieving a global energy consumption saving of around 1.5 kWh/kg Al.

3. Process Gases Energy and Alumina Heat-up Potential

The bath cavity reactions produce gases, in majority CO_2 and additionally CO, COS, HF, $NaAlF_4$ among other minor contributions. Detailed description of the cell mass and energy balance can be found in [14]. The gases leave the cavity through holes in the crust. Once fresh air and oxygen is available, combustion of CO and COS can take place. In addition, the open holes favour carbon airburn.

The amount of energy available to use in alumina preheat comes from the enthalpy of gases leaving the cavity at ~ 960 °C and from combustion processes:

- Considering the gas mix of the bath cavity composed of CO_2 and additionally CO, COS, HF, $NaAlF_4$ leaving at 960 °C carry ~ 0.4 kWh/kg Al of sensible heat;
- Combustion of anode carbon, commonly known as carbon airburn provides 0.4 – 0.5 kWh/kg Al of available energy;
- Combustion of CO provides 0.4 – 0.5 kWh/kg Al of available energy;
- Combustion of COS provides 0.02 – 0.05 kWh/kg Al of available energy.

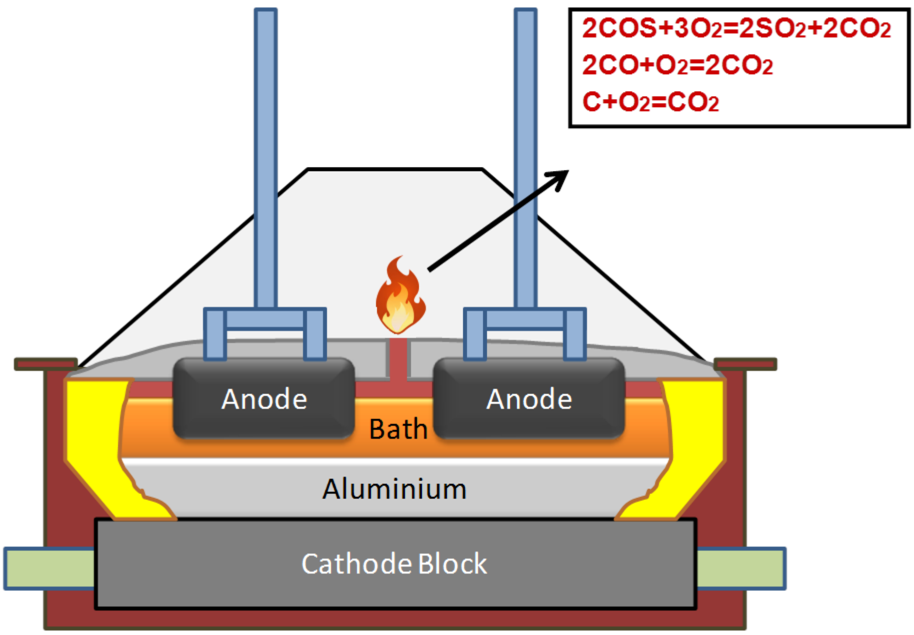

Figure 2. Exothermic reactions occurring at the open cell holes.

The total energy available is more than enough to fully preheat the alumina to 960 °C (theoretical requirement is 0.56 kWh/kg Al). However, some aspects of heat transfer, false air infiltration and material constraints of the superstructure limit the highest possible temperature of preheated alumina.

Estimations using the published calculation methodology for mass balance [14] would result in a total emission mass flow of 0.67 Nm^3/kg Al. The abovementioned combustion processes require that some potroom air is infiltrated to the superstructure in order to provide sufficient oxygen to the gas stream. Stoichiometric calculations estimate that a minimum of 120 % false air (with respect to the cavity gas mass flow, 0.80 Nm^3/kg Al) flow is necessary to fully burn C, CO and COS.

In traditional hooded cells the false air amount can be as high as 80 Nm^3/kg Al, which is a hundred times more than the necessary to combust the gases. Such high cold air flow induces high top heat loss by the cover and anode assembly surfaces. Heat transfer can be reduced by capturing the cell emissions in localized spots.

4. Heat Exchanger Design Options

The first attempt was to design a simple counter flow heat exchanger composed of concentric ducts. Inside the ducts a crust breaker is installed to guarantee that the hole remains open 100 % of the time. A small cap is placed over the hole, concentrating the gas collection. A controlled false air amount needs to be provided to the heat exchanger in order to combust the carbon based emissions before the main heat transfer zone.

After analyzing the simulation results (Section 5), it has been realized that the exchanger efficiency would be low due to the short distance between the alumina inlet and the crust opening (~ 0.6 m). Fins have been placed inside the alumina duct and also inside the gas duct space enabling a heat transfer enhancement (see Figure 3), allowing the alumina to be heated up to ~ 600 °C.

The design of the heat exchanger parts and its functioning is explained in Figure 3. The heat exchanger is embedded into the alumina hopper (2). The alumina feeding is activated by a pneumatic cylinder (3). Alumina passes through the alumina heating chamber (4) reaching the dosing device (6). A crust breaker (5) is necessary to guarantee the crust opening stability. When the pneumatic cylinder acts, the alumina falls into the discharging chute (7). A gas collection cap (8) is placed over the anode cover (9). It presents a vertical sliding degree of freedom allowing for the anode height variation during the anode life. The gas collection cap presents a controllable false air inlet (12). The hot gases evolving from anodes (10) and bath (11) are collected and directed in counter flow with regard to the alumina flow. The gases leave the heat exchanger at the top where a draft control valve with temperature sensor (1) is used to control the off gas temperature and mass flow.

The material selection for the heat exchanger construction must take into account the aggressive environment at the cell top. Due to the presence of combustion gases, including sulphur compounds, high temperature and oxygen from false air, a stainless steel with high chromium content should be selected. High temperature series stainless steel such as AISI 310 or AISI 330 might be necessary for the internal parts. The external parts are subjected to lower temperatures and AISI 316 steel maybe suitable, lowering the total structure cost. Additionally, all heat exchanger options should consider insulating the external surfaces of the heat exchanger body.

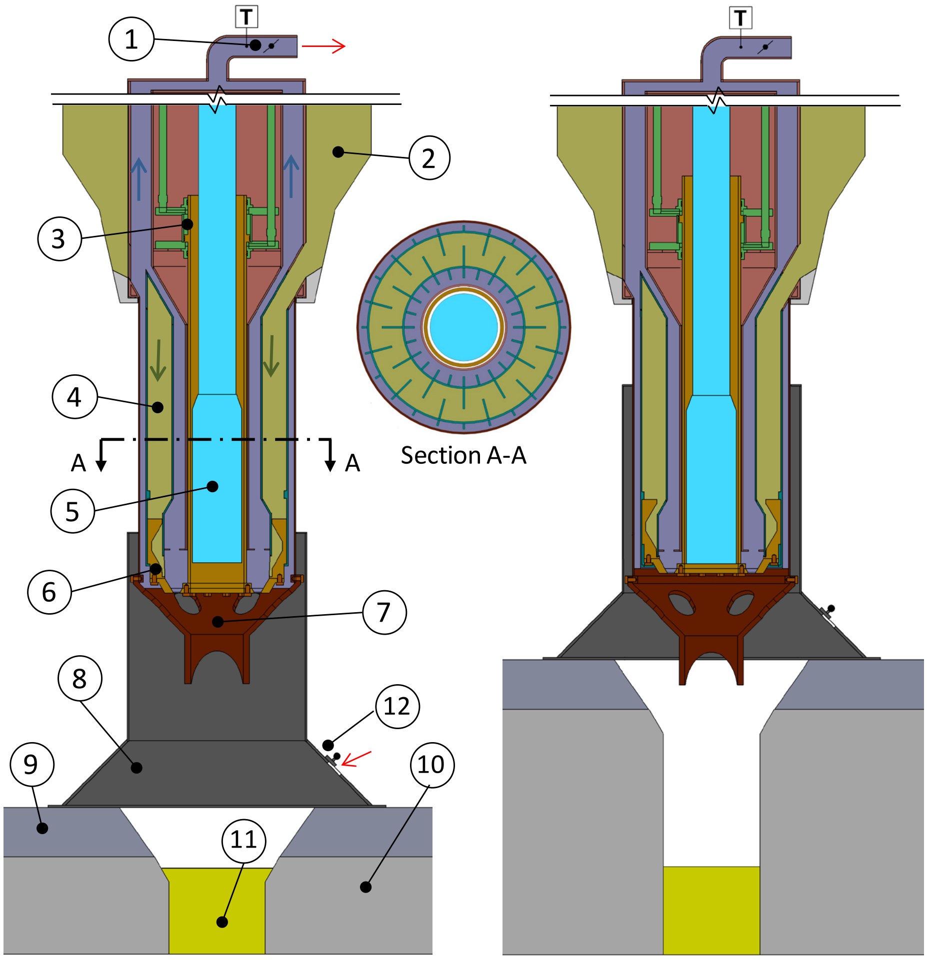

Figure 3. Counter flow heat exchanger with fins. Left: Exchanger positioned over butt anodes. Right: Exchanger positioned over new anodes.

5. Numerical Model Studies

A numerical model based on OpenFOAM CFD code was developed in order to study the prototype thermal efficiency and to determine its optimum dimensions. OpenFOAM is a Finite Volume based code, open software, largely used by researchers as a tool for virtual CFD testing. In the model, due to axisymmetry of the design, it is possible to model a 15 ° slice of the heat exchanger. The Figure 4 presents the mesh used in the base model along with indication of the boundary conditions used.

The main objective of the study is to assess the final bulk alumina temperature function of the exchanger height and diameters. In this article, detailed results for the base case will be presented. Afterwards, general temperature results for the height and diameter studies are also presented.

5.1 Base Case Results

Many solvers are available in OpenFOAM, depending on the physics included in the study. In this case the chtMultiRegionSimpleFoam.exe was chosen for the simulation. It is steady state buoyant solver for conjugate heat transfer problems. The gas is modelled with perfect gas properties, and the alumina is modelled as moving solid with a prescribed flow rate calculated from the electrolysis cell alumina consumption rate.
The boundary conditions are described below and indicated at Figure 4:

- At the bottom of the heat exchanger the gas enters the domain coming from the cell cavity. 960 °C is adopted as gas temperature. False air level is 3x the cell cavity gas flow. False air temperature is 100 °C;
- An additional false air inlet is placed at the side gap, with mass flow equal to 1x the gas flow from the cavity. False air temperature is at 100 °C;
- At the inlet region, a heat source representing the combustion of C, CO and COS is implemented. The source power is calculated by the methodology presented in [14];
- Alumina movement is considered continuous in the model; although in the real process a pulsed movement shall be observed. This approximation is quite acceptable because we are interested in the final alumina temperature before falling into the bath cavity;
- Wall heat transfer coefficient is applies at the external walls, h=10 W/m^{2}C at environment temperature of 100 °C;
- Alumina inlet temperature is 25 °C;
- The turbulence is modelled with the SST-komega model; it is a Reynolds averaged two equations model.

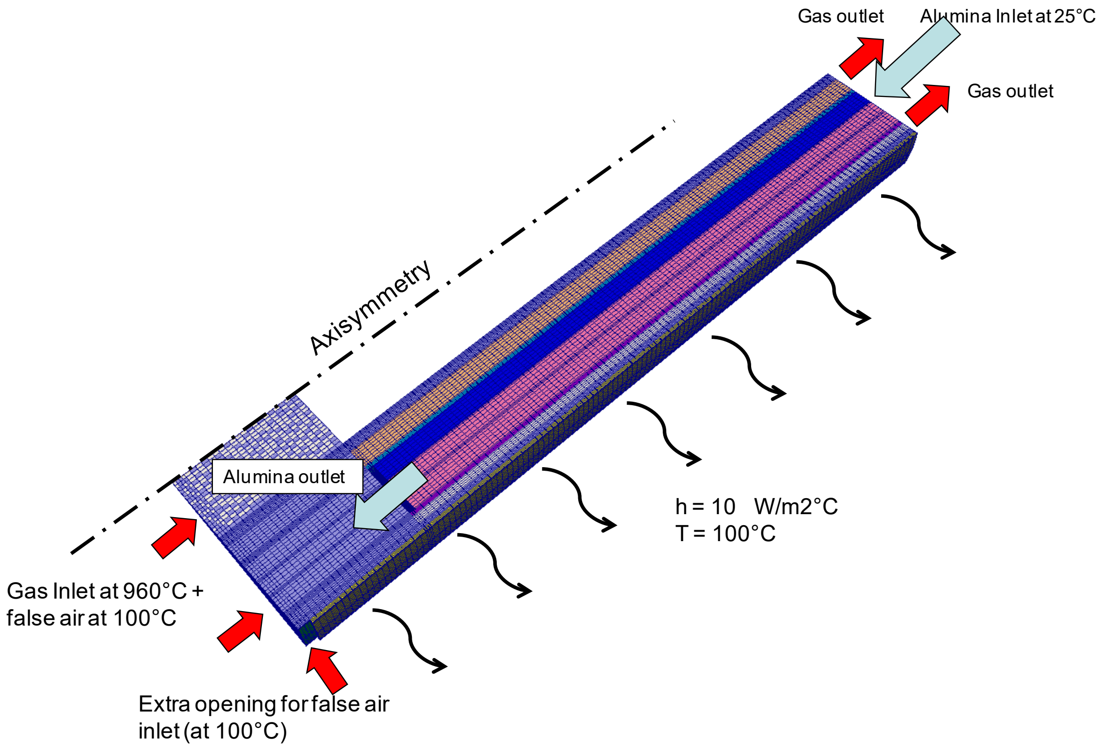

Figure 4. CFD mesh of the heat exchanger 15° slice used in the simulations.

The simulated gas flow and alumina temperature are shown in Figure 5. The fins are a very important feature to homogenise the alumina temperature and to improve the heat exchange. The numerical model is a valuable tool to optimize the fin numbers and shape.

The most important outcome of the model is shown in Figure 6. Final alumina temperature before falling into the bath is presented and the resulting averaged temperature is 582 °C.

The top temperature field, showing gas, alumina and steel parts of the heat exchanger is shown in Figure 7. While the alumina enters the heat exchanger at 25 °C, it can be observed that the steel parts present higher temperatures. The inner gas flow is hotter that the outer gas flow. The outer gas flow temperature is more influenced by the false air entering at the side opening over the cell crust.

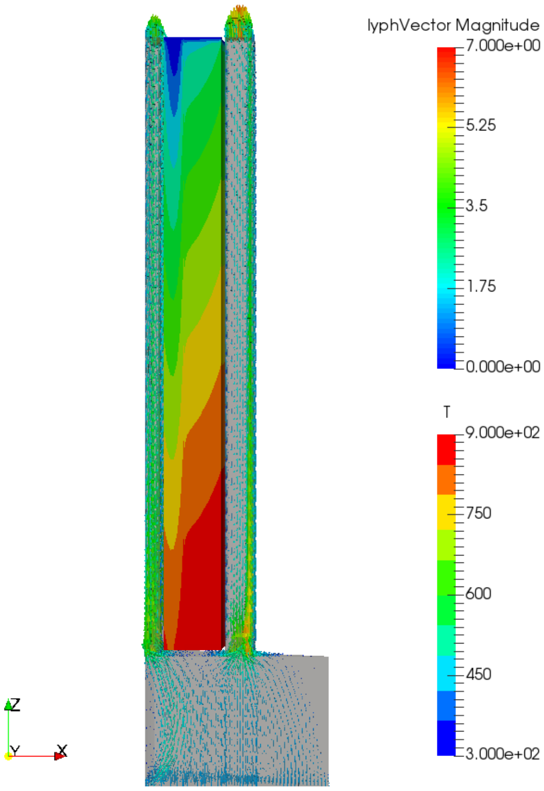

Figure 5. Gas velocity vectors [m/s] and alumina temperature in (K) inside the heat exchanger, left: plane cutting the inner side fin, right: plane cutting the outer side fin.

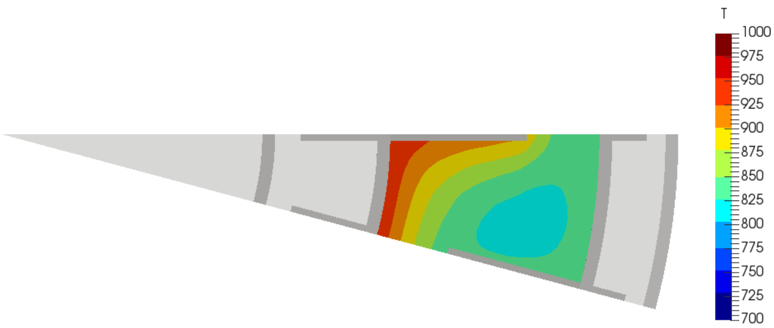

Figure 6. Bottom view of the final alumina temperature (K).

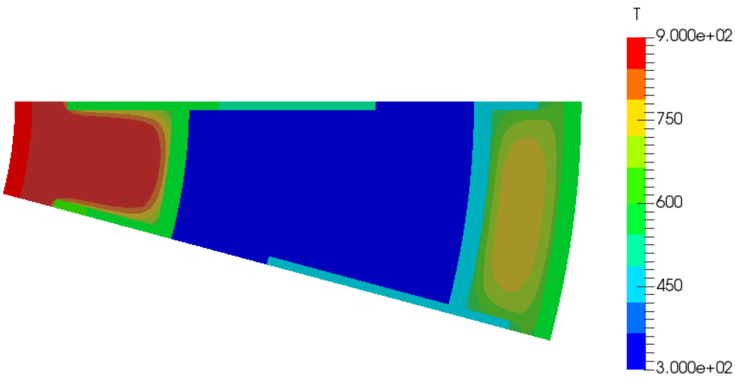

Figure 7. Temperature (K) at the top of the heat exchanger, alumina, steel and gas.

5.2 Alumina Duct Diameter Study

The influence of the alumina duct diameters was studied using the CFD model. Three sets of diameters were chosen and the main geometric parameters are shown in Table 1.

Table 1. Dimensions of diameter variation study models.

Case	Inner alumina duct diameter (mm)	Outer alumina duct diameter (mm)	Heat exchanger height (mm)	Alumina cross sectional area (cm^2)	Avg. alumina flow velocity (mm/s)
Narrow duct	213	285	500	282	0.341
Medium duct	199	295	500	372	0.257
Wide duct	183	305	500	468	0.204

In the thermal efficiency point of view, the effects of alumina duct cross sectional area increase are twofold:

- The alumina flow velocity decreases, increasing its residence time. This may increase the final alumina temperature;
- In the other hand, heat diffusion through alumina is slower at through a thicker alumina stream, obtained by a greater duct cross sectional area.

In the results, shown in Figures 8 and 9, it is shown that the final alumina temperature is almost not influenced by the cross sectional area, because the above mentioned effects cancel each other. The narrow alumina channel performs slightly better. However a too narrow channel is prone to present flowing problems like clogging; and therefore avoided. The prototype tests may give an indicative of the alumina flow difficulties related with cross sectional area.

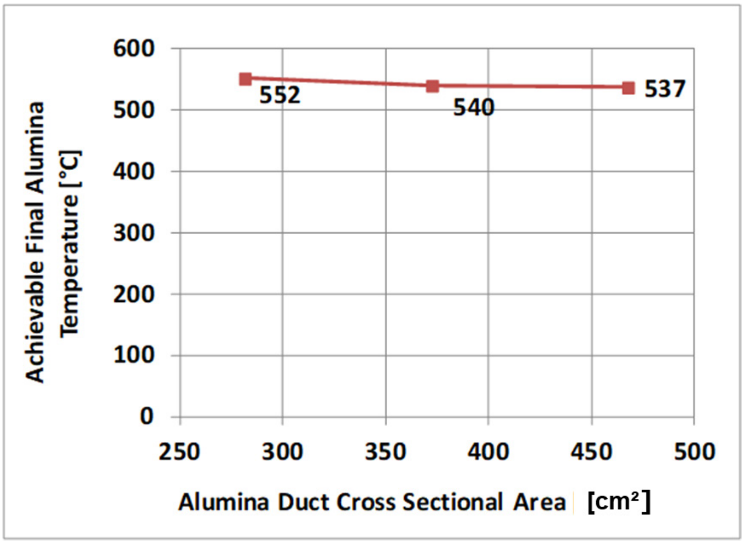

Figure 8. Averaged final alumina temperature (°C) function of duct cross sectional area (cm^2).

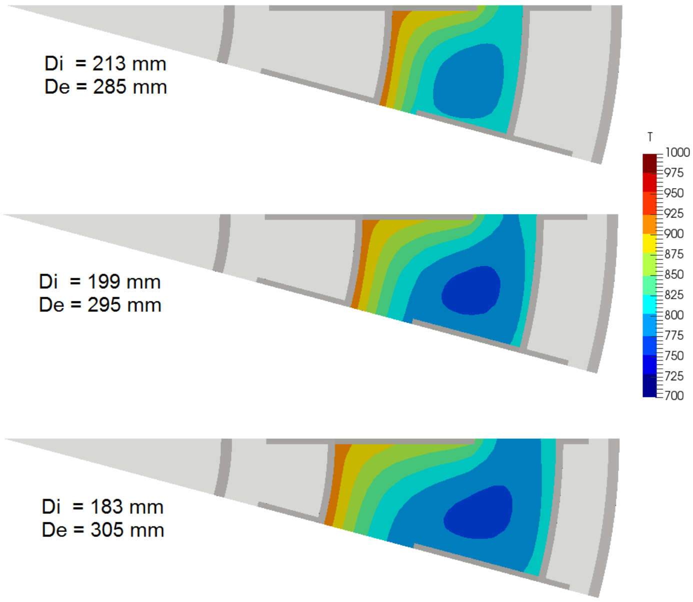

Figure 9. Final calculated alumina temperature (K), for 3 distinct combinations of alumina duct diameters.

5.3 Heat Exchanger Height Study

The heat exchanger height might be one of the most important design parameters in order to optimize thermal efficiency. Three height options were calculated by the model using the same diameters. The geometry parameters are specified in Table 2.

Table 2. Dimensions of height variation study models.

Case	Inner alumina duct diameter (mm)	Outer alumina duct diameter (mm)	Heat exchanger height (mm)	Alumina Cross sectional area (cm^2)	Avg. Alumina flow velocity (mm/s)
1	182	280	350	356	0.271
2	182	280	525	356	0.271
3	182	280	700	356	0.271

As expected, the results presented in Figure 10 and 11 show a progressive increase of the alumina final temperature with the exchanger height. The challenge is to implement the highest possible heat exchanger in the cell superstructure downstream to the alumina hopper.

Another aspect to consider for improving the heat exchanger efficiency is the number of feeders in the cell, or more specifically, the relation of electrical current per feeder. In the cases presented in this paper, a ratio of 50 kA per feeder is used. More feeders tend to be beneficial for the thermal efficiency as the residence time of alumina is increased.

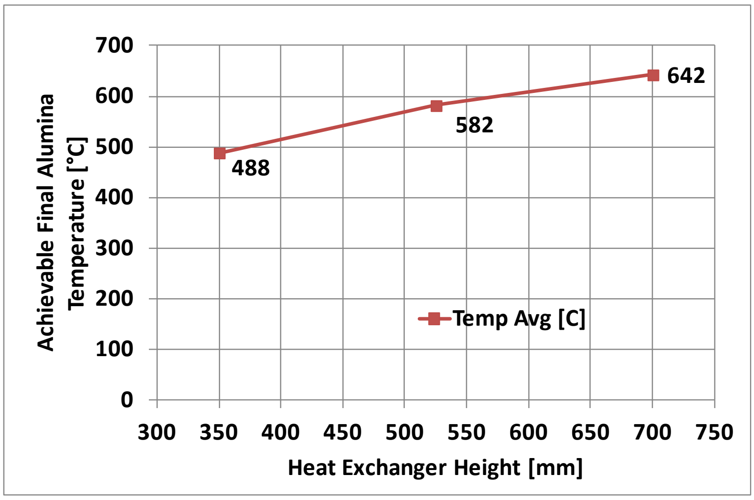

Figure 10. Averaged final alumina temperature (ºC) function of heat exchanger height (mm).

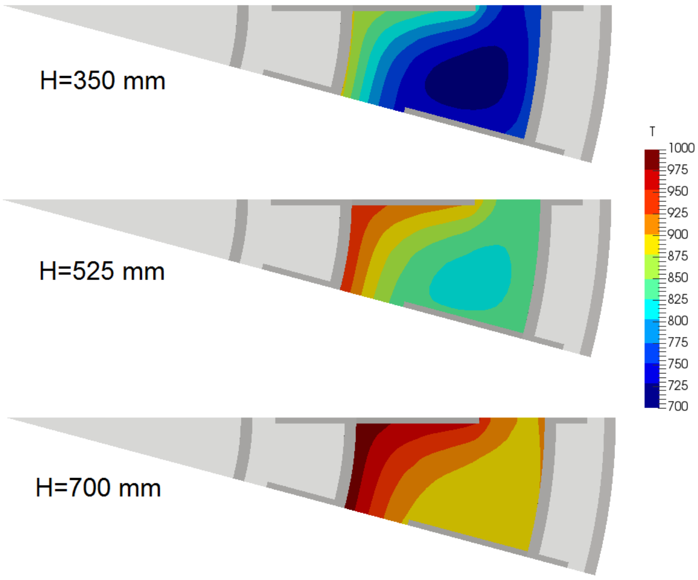

Figure 11. Final calculated alumina temperature (K), for 3 distinct heat exchanger heights.

6. Conclusions

An innovative alumina heat exchanger was presented and opens the possibility for substantial reduction in the cell energy consumption in the order to 1.2 – 1.5 kWh/kg Al, when considering all combined effects. The CFD models have shown that a preheat alumina temperature of 500 – 600 °C can be achieved.

The heat exchanger consists of concentric ducts where the alumina is heated up by the cell exhaust gases in counter flow with the alumina and by combustion of C, CO and COS. Fins are placed at gas side as well as at the alumina side in order to improve heat transfer capacity.

The following benefits are expected from the heat exchanger employment:

- Direct heat recovery through alumina preheat;

- Due to the alumina higher temperature feeding, better alumina dissolution and lower risk of sludge formation is expected;
- Possibility to reduce the electrolyte superheat by up to 50 %;
- Localized exhaust gas reduces the cell under hood temperature, reducing the global top heat losses.

In this paper, the importance of the heat exchanger height has been demonstrated. In new cell designs, the superstructure could be designed to allow more space for the exchanger, further optimizing energy recovery. Model results have also shown that the exchanger diameters present low impact on the heat recovery efficiency.

Despite the potential gains demonstrated in this article, some technical difficulties are expected in the practice. The gas collection cap can be damaged during anode replacement, increasing maintenance costs. The pair of anodes supporting the cap at upstream and at downstream have to be replaced at the same time in order to keep the cap properly aligned.

7. References

1. Geir Wedde, Anders Sørhuus, Waste Heat Recovery from Industrial Smelting Exhaust Gas, *TMS International Smelting Technology Symposium* 2012, 31-38.
2. Anders Sørhuus, Geir Wedde, Pot gas heat recovery and emission control, *Light Metals* 2009, 281-286.
3. Hadi Fanisalek, Mohsen Bashiri, Reza Kamali, Waste Heat Recovery Trial From Aluminum Reduction Cell Exhaust Gases, *TMS Energy Technology Proceedings* 2011, 65-75.
4. Amal Aljasmi et al., Heat Recovery from Aluminium Cells Based on Heat Pipe Technology, *11h Australasian Aluminium Smelting Technology Conference,* 6 - 11 December 2014, Dubai, UAE.
5. Yves Ladam, Asbjørn Solheim, Martin Segatz, and Odd-Arne Lorentsen, Heat Recovery from Aluminium Reduction Cells, *Light Metals* 2011, 393-398.
6. S. Kothari, A. F. A. Hoadley and D. J. Brennan, An Investigation of Anode Preheat on The Thermal Efficiency of a Hall-Heroult Reduction Cell, *7th Australasian Aluminium Smelting Technology Conference* 11 -16 November 2001, Melbourne, Australia.
7. Odd-Arne Lorentsen, Are Dyrøy, and Morten Karlsen, Handling CO_2eq from an Aluminum Electrolysis Cell, *Light Metals* 2009, 263-268.
8. Morten Karlsen et al., A Device for Collection of Hot Gas from an Electrolisys Process and a Method for Gas Collection with Said Device, Patent WO2010033037, 25 March 2008.
9. Martin Segatz et al., Hydro's Cell Technology Path towards Specific Energy Consumption below 12 kWh/kg, *Light Metals* 2016, 301-305.
10. Kellinghaus Hans Dipl Schulte et al., Anode change with heat recovery during aluminium fusion electrolysis, German Patent DE 4344036 A1, 29 June 29 1995.
11. Mathias Ovrom Sem, Method of Charging Aluminium Furnaces, Patent US 3,006,825, 31 October1961.
12. Patent US 3,371,026, Allan Jack Kiley and Harry T. Shiver, Electrolytic reduction cell with crustbreaking and ore feeding means, Reynolds Metals Company, 27 February 1968.
13. Ove Kobbeltvedt, Sverre Rolseth and Jomar Thonstad, The dissolution behaviour of alumina in cryolite bath on a laboratory scale and in point fed industrial cells, Light Metals 1996, 421-427.
14. Vanderlei Gusberti, Modelling the Mass and Energy Balance of Aluminium Reduction Cells, *PhD Thesis*, *University of New South Wales*, Australia, 2014.